Correlation between sinus rhythm deceleration zones and critical sites for localized reentrant atrial flutter: A retrospective multicenter analysis

Christopher E. Woods, MD, PhD, FHRS,[*] Amir A. Schricker, MD, MS, FHRS,[†]
Hemal Nayak, MD, FHRS,[‡] Ramesh Hariharan, MD,[§] Brady Stevens, BSE,[∥]
Agatha Kwasnik, BS,[¶] Nathan Shatz, BA,[∥] Lucas Suchomel, BSE,[∥] Ryan Moskovitz, BSE,[∥]
Jonathan Salcedo, MD, FHRS,[*] Roger Winkle, MD, FHRS,[†] Roderick Tung, MD, FHRS[#]

From the [*]*Department of Cardiology, California Pacific Medical Center, San Francisco, California,*
[†]*Department of Cardiology, Palo Alto Medical Foundation, Burlingame, California,* [‡]*Center for
Arrhythmia Care, Pritzker School of Medicine, University of Chicago, Chicago, Illinois,* [§]*University of
Texas, Houston, Texas,* [∥]*Abbott Laboratories, Abbott Park, Illinois,* [¶]*Boston Scientific, Natick,
Massachusetts, and* [#]*Banner Cardiovascular Center, The University of Arizona College of
Medicine-Phoenix, Phoenix, Arizona.*

BACKGROUND Atypical left atrial flutter (AFL) may be macroreentrant or spatially localized. The relationship between the critical isthmus (CI) for localized reentry with sinus rhythm (SR) conduction slowing has not been systematically examined.

OBJECTIVE To examine the correlation between CI sites for localized AFL (L-AFL) and deceleration zones (DZ) identified by isochronal late activation mapping (ILAM) during baseline rhythm.

METHODS Patients with localized AFL who underwent high-density activation mapping of both SR and AFL were retrospectively analyzed. L-AFL was defined as reentry restricted to 2 wall segments of the left atrium. CI was defined by activation mapping and sites of successful termination during ablation. DZ, defined as >3 isochrones within 1 cm radius during baseline rhythm, were correlated to the locations of the CI.

RESULTS Thirty-one consecutive patients that underwent detailed sinus rhythm and AFL high-density activation maps were analyzed at 3 centers. A mean 4060 ± 3275 and 6209 ± 8656 points were collected in ILAM and AFL activation maps, respectively. At least 1 DZ (1.7 ± 0.77) was identified in all patients. ILAM showed 3.27 ± 0.52 isochrones per DZ (168 ± 32 ms), and co-localized to CI sites at a distance of 6.7 ± 3 mm. A total of 34% ± 14% of the AFL cycle length was contained within 0.5 cm of the DZ.

CONCLUSIONS In patients with L-AFL, CI co-localized with DZ during baseline rhythm, suggesting that DZ mapping during SR may yield candidate targets for ablation as an adjunct to pulmonary vein isolation to prevent a subtype of AFL.

KEYWORDS Atypical atrial flutter; Conduction slowing; Electroanatomic mapping; Isochronal mapping; Reentry

(Heart Rhythm 0² 2022;3:279–287) © 2022 Heart Rhythm Society. Published by Elsevier Inc. This is an open access article under the CC BY-NC-ND license (http://creativecommons.org/licenses/by-nc-nd/4.0/).

Introduction

Atypical atrial flutters (AFL) in the left atrium (LA) may be macroreentrant or spatially localized after catheter ablation for atrial fibrillation and in patients with atrial cardiomyopathy.[1] Gaps in incomplete linear lesion sets are common mechanisms of iatrogenic AFL by creating narrow critical isthmus (CI) regions that help sustain reentry.[2] Ultra-high-density mapping of flutters with multielectrode catheters has facilitated rapid and precise delineation of AFL.[3,4] Whether atypical flutters occur as a result of an extent of fixed substrate abnormalities and conduction barriers or of functional reentry is incompletely understood.

Recently, an approach to mapping ventricular tachycardia by targeting deceleration zones (DZ), areas of sudden conduction velocity (CV) slowing during sinus rhythm (SR), has been shown to be effective at predicting CI sites, obviating the requirement for extensive homogenization.[5,6] Isochronal late activation mapping (ILAM) during SR allows for visual identification of regions of wavefront discontinuities with isochronal crowding, which may represent the most arrhythmogenic regions for reentry with a given substrate.

The role of conduction slowing during baseline rhythm for the development and maintenance of atypical AFL has not

Address reprint requests and correspondence: Dr Christopher E. Woods, California Pacific Medical Center, 1100 Van Ness 5th Floor, San Francisco, CA 94109. E-mail address: woodsc@sutterhealth.org; or Dr Roderick Tung, The University of Arizona College of Medicine-Phoenix, Banner University Medical Center-Phoenix, 755 E McDowell Rd, Phoenix, AZ 85006. E-mail address: rodericktung@arizona.edu.

KEY FINDINGS

- The relationship between the critical isthmus (CI) for localized reentry with sinus rhythm (SR) conduction slowing has not been systematically examined.

- CI sites for localized atypical flutter spatially co-localize to deceleration zones identified during SR.

- These data support the hypothesis that areas of localized atypical flutter can be predicted in SR.

been systematically investigated. We hypothesized that DZ can be identified during baseline rhythm in patients with localized flutter, and spatially co-localize with ablation termination sites. We performed a retrospective multicenter study among consecutive patients who underwent ultra-high-density mapping of the atria during both baseline rhythm prior to ablation and AFL to assess for spatial correlation between DZ and critical sites for reentry.

Methods
Study design and enrollment
The research reported in this paper adhered to the Helsinki Declaration guidelines. Informed written consent was waived by institutional review boards. Patients >21 years old referred for ablation of atypical left AFL were analyzed at the Mills-Peninsula Medical Center (Burlingame, CA), Sequoia Hospital (Redwood City, CA), University of Texas Houston (Houston, TX), and University of Chicago Medical Center (Chicago, IL). Localized AFL was defined as reentry restricted to less than 2 wall segments of the LA. The LA segments were allocated as anterior, septal, roof, lateral, posterior wall (dome), and vestibule (floor). Data analysis was retrospective and approved by the institutional review board at each institution.

Conduction slowing mapping during sinus rhythm
An overview of the procedural sequence is shown in Figure 1. To study conduction during SR and AFL, we only included patients who were in SR either spontaneously or after direct current cardioversion. Any patient that had delivery of radiofrequency during the procedure prior to obtaining both ILAM and AFL activation maps was excluded. If the sinus rate was slow or if there was significant ectopy, atrial pacing was employed to expedite mapping. A 20-pole (Livewire; Abbott Laboratories, Abbott Park, IL) or 10-pole (Inquiry, Abbott) catheter was inserted into the coronary sinus (CS). Intravenous heparin was infused to maintain activated clotting time >300 seconds. Following access to the LA via a transseptal approach, a 3-dimensional electroanatomic geometry was created with the mapping catheter.

High-density activation mapping of the atrium was performed with the EnSite Precision system (Abbott) using a grid catheter (HD Grid; Abbott) or the Rhythmia system (Boston Scientific, Natick, MA) using a mini-electrode

basket catheter (Orion; Boston Scientific). For EnSite Precision, the AutoMap feature, which automatically and rapidly collects a large number of points, was used; for Rhythmia, the default automated annotation was used. All atrial paced or SR maps were performed prior to any AFL mapping or ablation in this cohort. Local signals were automatically annotated at the maximum absolute value of the dV/dt with both electroanatomic mapping systems. All activation maps used a stable bipolar intracardiac electrogram reference, typically from an electrode pair of the CS catheter. A speed limit was set for all activation maps to only select points when the mapping catheter was in a stable position. We applied manual adjustments below the standard low-voltage thresholds, set at 0.1–0.5 mV on EnSite and 0.1–0.3 mV on Rhythmia, if a visualized low-voltage signal observed during real-time mapping fell below low-V ID and confidence mask threshold, respectively.

Activation was then visualized via isochronal analysis with the mapping window divided into 8 equal isochrones to standardize displays across all patients, as previously described.[5,6] DZ were defined as regions with isochronal crowding, where 3 or more isochrones were present within a 1 cm radius.

Atrial flutter mapping and ablation
Induction of AFL was done through rapid pacing with and without isoproterenol as needed. A surface electrocardiogram with a visible AFL wave was added to the mapping window to confirm stability of the reference electrogram relative to the AFL wave. The timing reference for the window was set at 60 ms before the onset of the most prominent flutter wave on the surface electrocardiogram, and the window spanned 95% of the tachycardia cycle length. Isochronal maps were created and were displayed as 8 equal time intervals, with the AFL circuit delineated by tracing the leading edge of each color.

CI sites were identified as areas with significant conduction slowing, similarly defined by isochronal crowding (>3 isochrones within a 1 cm radius), and where ablation terminated the arrhythmia. Ablation was performed during AFL targeting the narrowest portion of the region exhibiting maximal conduction slowing (isochronal crowding), confirmed to have long-duration fractionated signals. Ablation was performed using an open irrigated ablation catheter (Tacticath; Abbott Laboratories or IntellaNav; Boston Scientific) at 35–50 watts. The procedural endpoint was noninducibility of AFL. All patients also underwent pulmonary vein isolation (PVI) if pulmonary vein conduction was present.[7]

Correlation between DZ and CI
The CI of the AFL was analyzed and compared with the DZ identified on conduction slowing mapping during SR. The region of maximal crowding in each map was annotated by a 1 cm line in the direction of conduction, and the distance between the center of these lines was measured using the incorporated software measurement tool to quantify the extent of
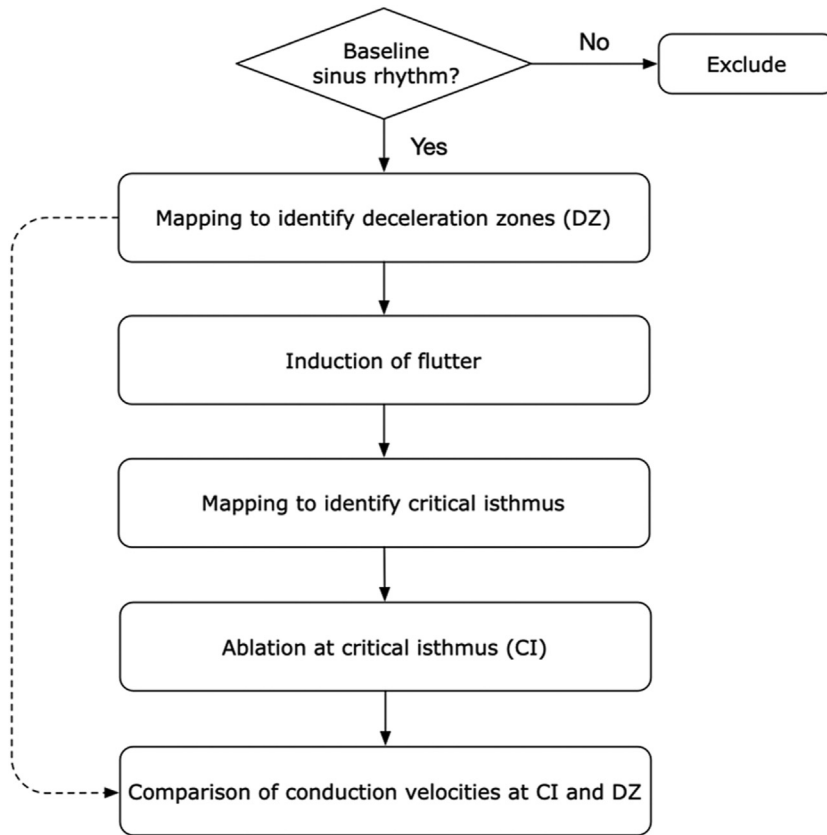
Figure 1   Procedural flow for mapping to compare baseline and tachycardia rhythms. Patients were included in this study if they presented in—or were able to be cardioverted to—sinus rhythm.

spatial co-localization (Figure 2). The correlation between the DZ and CI was validated by core lab. A clinical CV was estimated using a single-vector approach by measuring

distance propagated perpendicular to the isochronal lines over a 1 cm distance at maximal isochronal crowding during sinus/paced rhythm and flutter. A reference CV within
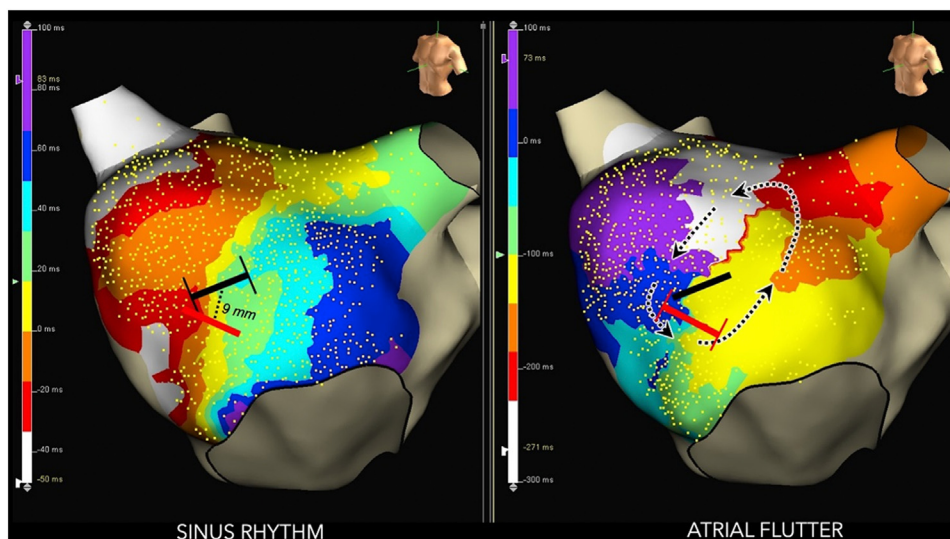

Figure 2   Co-localization between isochronal crowding during sinus rhythm and slow conduction at critical isthmus during reentry. Ultra-high-density map during sinus isochronal late activation mapping (left) and local activation time during atrial flutter (right). For conduction velocity estimation and co-localization, measurements were made over 1 cm perpendicular to isochronal crowding at deceleration zone (left) and critical isthmus (right). Red line shows region of measurements in atrial flutter, and black line shows region of measurements made in sinus. The distance between the center of the maximal conduction slowing during sinus rhythm and flutter is 9 mm.

Table 1 Patient baseline characteristics

Patient	Age/sex	Structural disease	Previous history	LA size (mm)	DZ mapping rhythm	Termination site	Distance between DZ and term site (mm)	Voltage at DZ (mV)
1	64/M	No	Persistent AF, limb-girdle muscular dystrophy	34	Sinus	LA AW	8	0.28
2	82/M	No	Persistent AF, PVI	50	Sinus	PW	7	0.08
3	55/M	No	Persistent AF, PVI	41	Sinus	LIPV	7	0.17
4	68/F	No	Persistent AF, PVI	41	Sinus	LA AW	5	0.07
5	56/M	No	Persistent AF, MV endocarditis, MVR, maze	40	Sinus	LA septum	7	0.39
6	64/F	No	Persistent AF, PVI	58	HRA pacing	MA	7	0.22
7	72/F	Yes	Persistent AF, DCM, PVI	58	HRA pacing	LA AW	0	0.21
8	74/M	No	Persistent AF, PVI and rotor ablation	50	HRA pacing	PW	4	0.33
9	73/M	No	Persistent AF, PVI	44	HRA pacing	LA AW	1	0.18
10	77/M	Yes	Persistent AF, MVR, maze, TMVR	48	HRA pacing	LA floor	8	0.21
11	64/F	Yes	Persistent AF, RHD, AVR, PVI	53	Sinus	LA septum	8	0.15
12	69/M	No	Persistent AF, PVI	67	HRA pacing	PW	4	0.20
13	68/M	No	Persistent AF, PVI	35	HRA pacing	LA AW	5	0.28
14	74/M	Yes	Persistent AF, PVI, MVR	57	HRA pacing	LA AW	4	0.23
15	76/F	No	Persistent AF	40	CS pacing	LA AW	12	0.35
16	65/M	No	Persistent AF	50	Sinus	LA AW	6	0.72
17	74/M	No	Persistent AF, PVI, MVR	50	CS pacing	PW	9	0.06
18	58/M	No	Persistent AF, AF	62	HRA pacing	LA AW	8	2.3
19	54/M	No	Persistent AF, MVR, maze	47	Sinus	PW	11	0.64
20	44/M	Yes	Persistent AF congenital AVB s/p PPM, history of PDA s/p closure, s/p CTI flutter	52	Sinus	LA septum	2	0.12
21	62/M	No	Persistent AF, PVI	NA	CS pacing	PW	7	0.15
22	77/M	No	Persistent AF, PVI	NA	CS pacing	LA AW	12	0.13
23	69/M	Yes	Persistent AF, HCM	48	CS pacing	MA	10	0.09
24	25/M	No	WPW, PVI	40	CS pacing	PW	7	0.08
25	74/M	No	Persistent AF, PVI	40	CS pacing	LA AW	0	0.43
26	70/M	Yes	Persistent AF, CAD/PVI	48	CS pacing	PW	5	0.21
27	68/M	No	Persistent AF, PVI	51	CS pacing	LA AW	16	0.2
28	65/M	No	Persistent AF, PVI	NA	HRA pacing	LA AW	8	0.13
29	72/M	No	Persistent AF PVI	NA	Sinus	LA AW	4	0.5
30	71/F	No	Persistent AF	35	CS pacing	PW & LA AW	10	0.4
31	55/M	No	Persistent AF maze	57	Sinus	PW	8	0.18
Mean ± SD	65 ± 11			48 ± 8			6.7 ± 3	0.31 ± 0.4

AF = atrial fibrillation; AVB = atrioventricular block; AVR = aortic valve replacement; CAD = coronary artery disease; CS = coronary sinus; CTI = cavotricuspid isthmus; DCM = dilated cardiomyopathy; DZ = deceleration zone; HCM = hypertrophic cardiomyopathy; HRA = high right atrium; LA = left atrium; LA AW = left atrial anterior wall; LIPV = left inferior pulmonary vein; MA = mitral annulus; MV = mitral valve; MVR = mitral valve replacement; PDA = patent ductus arteriosus; PVI = pulmonary vein isolation; PW = posterior wall; RHD = rheumatic heart disease; s/p = status post; TMVR = transcatheter mitral valve replacement; WPW = Wolff-Parkinson-White.

normal atrial myocardium (defined as >1 mV) was similarly made during each case.

Data analysis

Continuous data were described as mean ± standard deviation. Categorical data are summarized with frequency counts and percentages. Statistical significance was compared with the Student *t* test for independent samples. A 2-tailed probability of $P \leq .05$ was considered statistically significant. *P* values are reported.

Results

Left atrial procedures were screened between June 2018 and January 2020 for atypical AFL. Thirty-one patients with localized left AFL who presented in SR were analyzed.

Patient demographics

Baseline patient characteristics are shown in Table 1. Patients were aged 65 ± 11 years and with left atrial size 48 ± 8 mm. Six (19%) patients were women. Twenty-four (77%) had undergone a previous catheter ablation and 4 (11%) had a maze

Table 2   Characteristics of sinus deceleration zones and atrial flutter critical isthmuses

Deceleration zone	
Baseline window (ms)	168 ± 32
Duration of signal at DZ (ms)	103 ± 30
# of isochrones per DZ	3.3 ± 0.52
# of DZs per chamber	1.7 ± 0.77
Average voltage (mV) at DZ	0.31 ± 0.4
Average points used	Rhythmia 7898 ± 3410
	EnSite 2251 ± 945
Atrial flutter	
TCL (ms)	294 ± 46
Duration of signal at DZ (ms)	131 ± 34
% TCL localized to critical isthmus	34% ± 14%
Average points used	Rhythmia 15,250 ± 11,432
	EnSite 2250 ± 770
Mapping time per flutter (min)	12 ± 6
RF time to termination (s)	41 ± 30
Distance between AFL critical isthmus and deceleration zone (mm)	6.7 ± 3

AFL = atrial flutter; DZ = deceleration zone; RF = radiofrequency; TCL = tachycardia cycle length.

procedure. Seven (22%) patients had structural heart disease. A total of 32 AFL were mapped in 31 patients.

Characteristics of baseline rhythm mapping and deceleration zones

Baseline mapping was done during SR (n = 11), high right atrial pacing (n = 10), or CS distal pacing (n = 11) (Table 1). Only 1 wavefront of baseline activation was investigated per case. Pacing was used to facilitate more rapid collection. Pacing location was at the discretion of the operator. The average point density per baseline map was 2251 ± 945 with EnSite and 7898 ± 3410 with Rhythmia (Table 2). The average mapped window was 168 ± 32 ms.

Figure 3 and Supplemental Video 1 show examples of ILAM with a DZ map correlation with reentrant AFL, with corresponding electrograms. (Supplemental Figure 1 demonstrates electrogram automated annotation in more detail). Figure 3 shows the DZ, located along the posterior wall, with electrograms showing an area of slowing along with an isoelectric segment consistent with a line of block. Similarly, Figure 4 shows a DZ and slowing along with localized reentry, at the mitral annulus. There were 3.3 ± 0.5 isochrones contained in each DZ (Table 2). The average number of DZ per patient was 1.7 ± 0.8 (Table 2). The average duration of signal at DZ was 103 ± 30 ms.

Characteristics of atrial flutter mapping

A total of 32 distinct flutters were identified. One patient had 2 DZ and 2 flutters induced corresponding to each (patient 30). Mean tachycardia cycle length was 294 ± 46 ms. Complete mapping of the AFL tachycardia cycle length was achieved with 2250 ± 770 points with EnSite (n = 29) and 15,250 ± 11,432 points with Rhythmia (n = 8) (Table 2). Figure 3 illustrates an AFL as well in this patient. AFL was induced from that area,
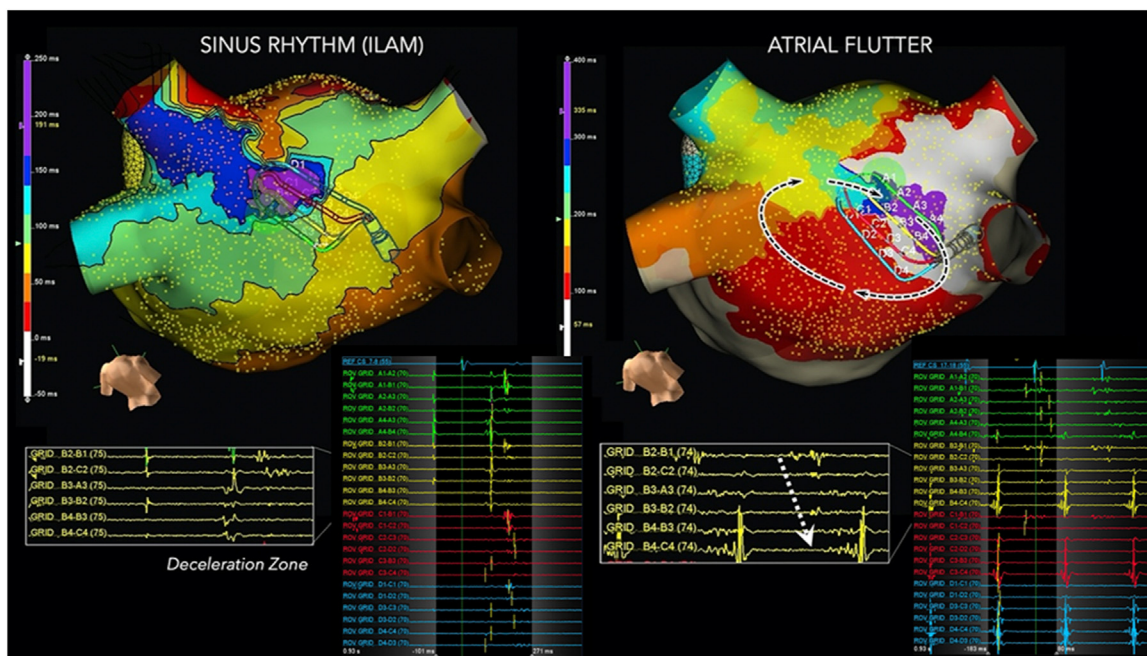

Figure 3   Correlation between isochronal late activation mapping (ILAM) deceleration zone (DZ) and atrial flutter in the left atrial posterior wall. Ultra-high-density ILAM during sinus rhythm and activation mapping during atrial flutter. During sinus, isochronal crowding, demonstrated by 3 isochronal colors (yellow to purple), are activated in a localized region of the primary DZ (left panel, HD-GRID location). Corresponding electrograms (EGMs) in this DZ during sinus rhythm show abrupt widening with split and fractionated EGM components, indicating abrupt conduction slowing across B2B4 splines (yellow EGMs). During atrial flutter (right panel), the entire circuit activation was mapped, demonstrating localized clockwise reentry, induced with presumed relief of unidirectional block at DZ. EGM annotation is shown in insets for DZ and atrial flutter for automated mapping. Ablation at this critical isthmus site, which co-localized with the DZ, terminated the flutter.
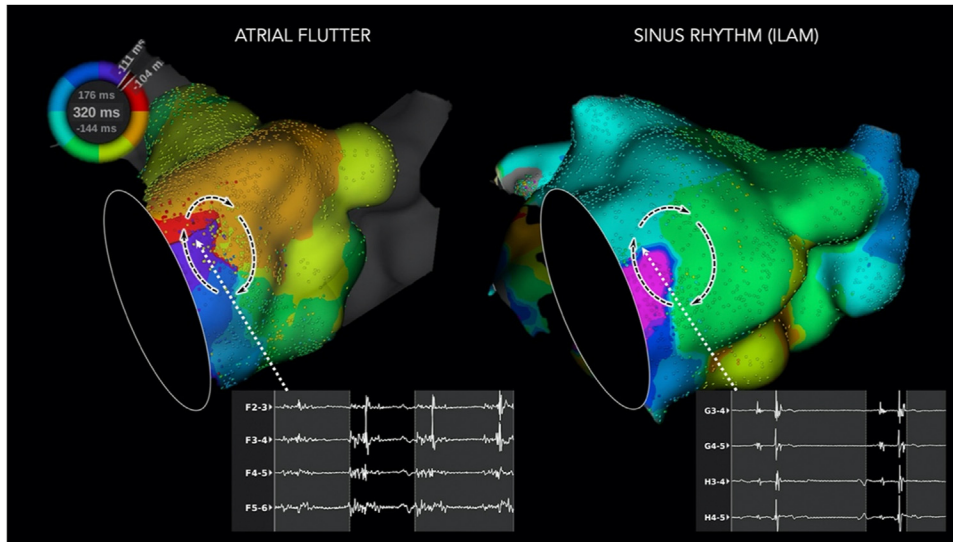
Figure 4 Correlation between isochronal late activation mapping (ILAM) and atrial flutter at the inferior mitral annulus. Ultra-high-density ILAM during sinus rhythm revealing isochronal crowding and abrupt conduction slowing, indicating a deceleration zone at the mitral annulus. Activation mapping during atrial flutter revealed localized clockwise reentry at the same site as the deceleration zone.

demonstrating slowing around the line of block for localized reentry, suggesting unidirectional functional block was relieved. The CI area contained 3.8 ± 1.0 isochrones. Ablation at the CI, which corresponded to the DZ location, promptly terminated the AFL. (See Supplemental Video 2 for AFL propagation movie).

Mean flutter mapping time was 12 ± 6 minutes. Characteristics of the flutter termination sites are described in
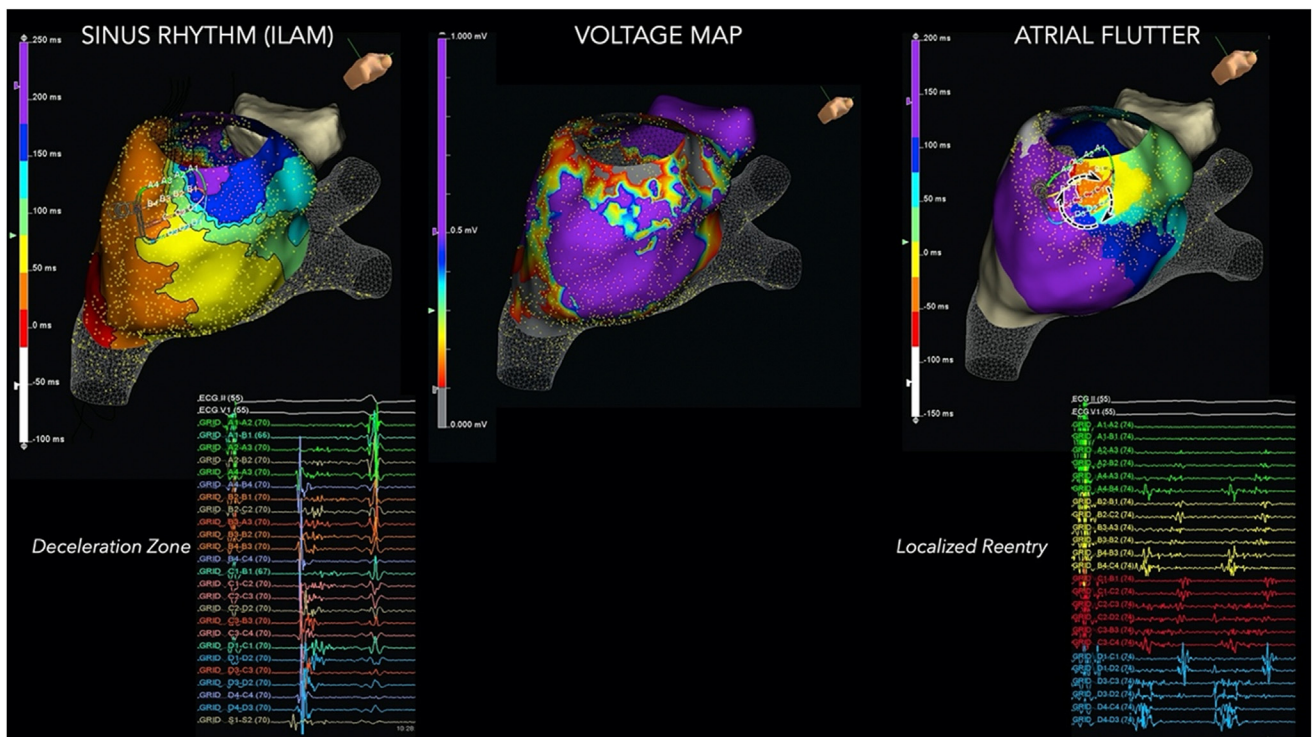
Figure 5 Comparison of isochronal late activation mapping (ILAM), atrial flutter mapping, and structural substrate mapping. Ultra-high-density map during sinus ILAM (left) with electrograms at deceleration zone (DZ), voltage map (middle) at the inferior mitral annulus, and mitral annular atrial flutter activation map (right) with electrograms at critical isthmus. Voltage scale 0.1–1.0 mV. Termination site of atrial flutter co-localized with the DZ, which corresponded with a low-voltage area on voltage mapping.
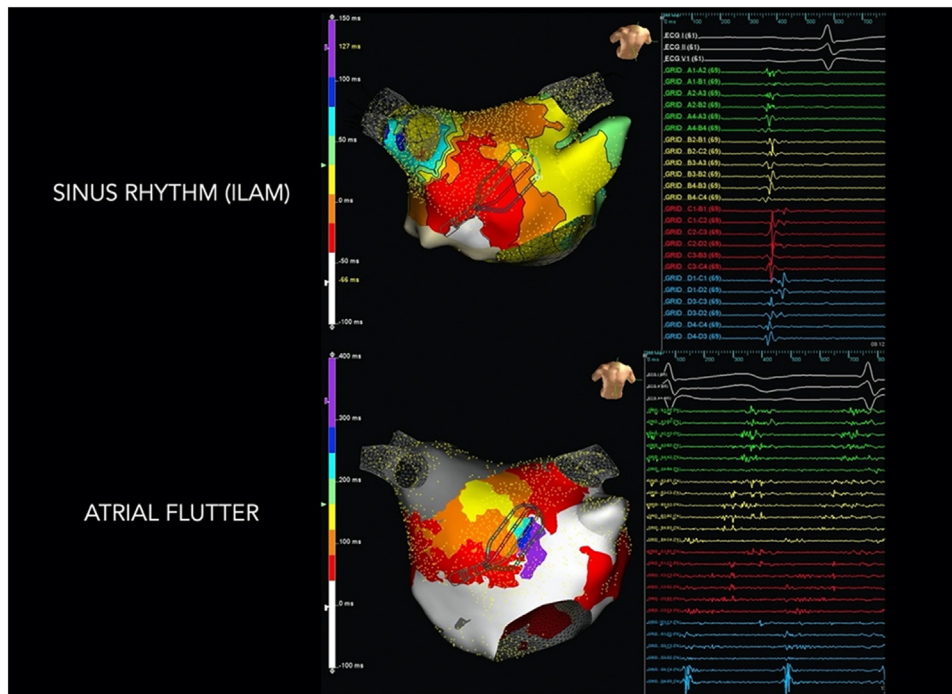
Figure 6   Arrhythmogenicity of anterior wall deceleration zone with subsequent critical isthmus during repeat ablation procedure. Ultra-high-density map during sinus isochronal late activation mapping (top left) with electrograms at deceleration zone (top right), and atrial flutter activation map with electrograms at critical isthmus (bottom row). The deceleration zone identified at the index pulmonary vein isolation ablation was not ablated and was co-localized to the critical isthmus of the atypical flutter that occurred 8 months later.

Table 1. Most AFLs were dependent to the LA anterior wall (43%) or the posterior wall (25%) (Table 1). Ablation was performed at the CI as defined by activation mapping and, in 1 patient, entrainment mapping. The mean duration of radiofrequency required for tachycardia termination was 41 ± 30 seconds (Table 2).

Correlation of atrial flutter CI with DZ

Figure 2 shows DZ and AFL at the LA anterior wall, with co-localization and velocity measurements demonstrated. AFL CI spatially co-localized with DZ, with a mean distance of 6.7 ± 3 mm (Tables 1 and 2). Critical slowing was observed in both DZ mapping and CI (Table 2). The substantive slowing at the DZ or CI led to $34\% \pm 14\%$ of the AFL cycle length being contained in the 0.5 cm on either side of the CI, with an average duration of signal there of 131 ± 34 ms in AFL (Table 2). Estimates of CV as a mapping tool were made perpendicular to the maximal region of isochronal crowding at the DZ and CI. CV within normal regions were estimated at 1.1 ± 0.24 m/s, 0.14 ± 0.05 m/s for the DZ, and 0.11 ± 0.06 m/s for the CI in AFL. The DZ and CI were significantly slower than normal CV by 90% ($P <$ e-29).

Conduction slowing corresponded to low-voltage regions (Table 1 and Figure 5). Substrate mapping in DZ and CI demonstrated scar, with average DZ voltage for the cohort 0.31 ± 0.4 mV (Tables 1 and 2).

Discussion

The major finding from this retrospective multicenter analysis is that CI sites for localized AFL spatially co-localize to DZ identified during SR. AFL circuits can be clinically delineated with high-density multielectrode mapping on all commercially available mapping platforms.[3,4] Localized reentrant patterns are amenable to rapid termination during radiofrequency application and often involve low-voltage regions with fractionated electrogram components during SR.[8,9] While voltage mapping reflects structural abnormalities, functional mapping of SR propagation has been shown to identify wavefront discontinuities that frequently correlate with critical sites for reentrant ventricular tachycardia.[5,10] Similarly, we demonstrate that most CI regions correlate with DZ during baseline rhythm. The co-localization of DZ and CI suggest that a critical degree of CV slowing is present during SR (ie, fixed), and localized reentry in such patients is not purely functional.

Atrial tachycardias and atypical flutters after left atrial ablation are common, often necessitating repeat ablation procedures.[11] In addition, atypical and multiple AFL can be complex, and despite high-resolution mapping, the presence of multiple flutters increases procedural time. A physiologically guided substrate approach to enhance atypical AFL ablation during SR is desirable. As such, strategies

such as empiric linear lesion sets have been proposed to mitigate the risk for reentrant arrhythmias[12] but have not consistently shown clinical benefit.[13] At present, empiric ablation targets outside of PVI have not been consistently demonstrated, and methods to predict regions that are more prone to reentry have not been established. Empiric ablation of low-voltage regions to target fibrosis has been proposed, with inconsistent results,[14–16] although more extensive fibrosis has been associated with higher rates of recurrence.[17] A clinical question is whether DZ can predict subsequent flutters, and whether adjunctive focused ablation of these DZ may reduce recurrence rates of atrial arrhythmias after PVI. Figure 6 shows a case of a PVI procedure at which a DZ was identified but not ablated. Eight months later the same patient developed AFL with a CI at the site of the DZ identified during the index PVI. These data suggest that specific targeting of arrhythmogenic zones can be performed during SR without the requirement of repeated inductions of AFL, and a strategy of targeting DZs empirically at index atrial fibrillation warrants study prospectively to see if it can reduce AFL recurrence.

Study limitations

Macroreentrant mitral and roof-dependent flutters without apparent conduction slowing were not included in this analysis that focused on localized reentry. The influence of prior ablation and lesion sets, which were not fully retrievable from this retrospective cohort, cannot be discerned from this analysis. The impact of the wavefront of activation cannot be assessed from this analysis, as we did not perform systematic multiple wavefront protocols in this retrospective series. The specificity of these wavefront discontinuities is incompletely addressed in this retrospective series, and prospective studies with protocol-mandated remapping and implantable loop recorders may more optimally identify recurrences. Reentrant circuits can be terminated with radiofrequency ablation at multiple locations. One of the major limitations of the present study was that entrainment mapping was also not used to confirm sites critical for reentry. Rather, interruption and termination of tachycardia during ablation was prioritized as the criteria for a site-critical for reentry, delivered in the slow conduction channels based on activation mapping. Lastly, retrospective analysis and lack of blinding may introduce selection bias with regard to correlation between DZ and critical sites. The sensitivity and specificity of DZ for isthmus sites requires prospective evaluation.

Conclusion

Critical sites for localized reentrant AFL correlated and spatially co-localized to DZ during SR. Studies targeting empiric ablation of these regions prospectively to investigate reduction in subsequent AFL recurrence are warranted.

Appendix
Supplementary data
Supplementary data associated with this article can be found in the online version at https://doi.org/10.1016/j.hroo.2022.03.003.

References

1. Chugh A, Oral H, Lemola K, et al. Prevalence, mechanisms, and clinical significance of macroreentrant atrial tachycardia during and following left atrial ablation for atrial fibrillation. Heart Rhythm 2005;2:464–471.
2. Chae S, Oral H, Good E, et al. Atrial tachycardia after circumferential pulmonary vein ablation of atrial fibrillation: mechanistic insights, results of catheter ablation, and risk factors for recurrence. J Am Coll Cardiol 2007; 50:1781–1787.
3. Luther V, Sikkel M, Bennett N, et al. Visualizing localized reentry with ultra-high density mapping in iatrogenic atrial tachycardia: beware pseudo-reentry. Circ Arrhythm Electrophysiol 2017;10:e004724.
4. Patel AM, d'Avila A, Neuzil P, et al. Atrial tachycardia after ablation of persistent atrial fibrillation: identification of the critical isthmus with a combination of multielectrode activation mapping and targeted entrainment mapping. Circ Arrhythm Electrophysiol 2008;1:14–22.
5. Aziz Z, Shatz D, Raiman M, et al. Targeted ablation of ventricular tachycardia guided by wavefront discontinuities during sinus rhythm: a new functional substrate mapping strategy. Circulation 2019;140:1383–1397.
6. Raiman M, Tung R. Automated isochronal late activation mapping to identify deceleration zones: rationale and methodology of a practical electroanatomic mapping approach for ventricular tachycardia ablation. Comput Biol Med 2018;102:336–340.
7. Calkins CH. 2012 HRS/EHRA/ECAS Expert Consensus Statement on Catheter and Surgical Ablation of Atrial Fibrillation: recommendations for patient selection, procedural techniques, patient management and follow-up, definitions, endpoints, and research trial design. Heart Rhythm 2012;9:632–696.
8. Kitamura T, Takigawa M, Derval N, et al. Atrial tachycardia circuits include low voltage area from index atrial fibrillation ablation relationship between RF ablation lesion and AT. J Cardiovasc Electrophysiol 2020;31:1640–1648.
9. Jadidi A, Nothstein M, Chen J, et al. specific electrogram characteristics identify the extra-pulmonary vein arrhythmogenic sources of persistent atrial fibrillation - characterization of the arrhythmogenic electrogram patterns during atrial fibrillation and sinus rhythm. Sci Rep 2020;10:9147.
10. Ciaccio EJ, Tosti AC, Scheinman MM. Relationship between sinus rhythm activation and the reentrant ventricular tachycardia isthmus. Circulation 2001;104:613–619.
11. Sawhney N, Anousheh R, Chen W, Feld GK. Circumferential pulmonary vein ablation with additional linear ablation results in an increased incidence of left atrial flutter compared with segmental pulmonary vein isolation as an initial approach to ablation of paroxysmal atrial fibrillation. Circ Arrhythm Electrophysiol 2010;3:243–248.

12. Pappone C, Manguso F, Vicedomini G, et al. Prevention of iatrogenic atrial tachycardia after ablation of atrial fibrillation: a prospective randomized study comparing circumferential pulmonary vein ablation with a modified approach. Circulation 2004;110:3036–3042.

13. Verma A, Jiang CY, Betts TR, et al. Approaches to catheter ablation for persistent atrial fibrillation. N Engl J Med 2015;372:1812–1822.

14. Yang B, Jiang C, Lin Y, et al. STABLE-SR (electrophysiological substrate ablation in the left atrium during sinus rhythm) for the treatment of nonparoxysmal atrial fibrillation: a prospective, multicenter randomized clinical trial. Circ Arrhythm Electrophysiol 2017;10:e005405.

15. Kottkamp H, Berg J, Bender R, Rieger A, Schreiber D. Box isolation of fibrotic areas (BIFA): a patient-tailored substrate modification approach for ablation of atrial fibrillation. J Cardiovasc Electrophysiol 2016;27:22–30.

16. Jadidi AS, Lehrmann H, Keyl C, et al. Ablation of persistent atrial fibrillation targeting low-voltage areas with selective activation characteristics. Circ Arrhythm Electrophysiol 2016;9:e002962.

17. Marrouche NF, Wilber D, Hindricks G, et al. Association of atrial tissue fibrosis identified by delayed enhancement MRI and atrial fibrillation catheter ablation: the DECAAF study. JAMA 2014;311:498–506.